

UV-B-Induced Inhibition of Photosystem II Electron Transport Studied by EPR and Chlorophyll Fluorescence. Impairment of Donor and Acceptor Side Components[†]Imre Vass,^{*,‡} László Sass,[‡] Cornelia Spetea,[‡] Alexandra Bakou,[§] Demetrios F. Ghanotakis,[§] and Vasili Petrouleas^{||}

Institute of Plant Biology, Biological Research Center, Szeged, Hungary, Department of Chemistry, University of Crete, Iraklion, Greece, and Institute of Materials Science, National Center for Scientific Research "Demokritos", 15310 Athens, Greece

Received December 28, 1995; Revised Manuscript Received April 30, 1996[®]

ABSTRACT: Inhibition of photosystem II electron transport by UV-B radiation has been studied in isolated spinach photosystem II membrane particles using low-temperature EPR spectroscopy and chlorophyll fluorescence measurements. UV-B irradiation results in the rapid inhibition of oxygen evolution and the decline of variable chlorophyll fluorescence. These effects are accompanied by the loss of the multiline EPR signal arising from the S₂ state of the water-oxidizing complex and the induction of Signal II_{fast} originating from stabilized Tyr-Z⁺. The EPR signals from the Q_A⁻Fe²⁺ acceptor complex, Tyr-D⁺, and the oxidized non-heme iron (Fe³⁺) are also decreased during the course of UV-B irradiation, but at a significantly slower rate than oxygen evolution and the multiline signal. The decrease of the Fe³⁺ signal at high *g* values (*g* = 8.06, *g* = 5.6) is accompanied by the induction of another EPR signal at *g* = 4.26 that arises most likely from the same Fe³⁺ ion in a modified ligand environment. UV-B irradiation also affects cytochrome *b*-559. The *g* = 2.94 EPR signal that arises from the dark-oxidized form is enhanced, whereas the light inducible *g* = 3.04 signal that arises from the photo-oxidizable population of cytochrome *b*-559 is diminished. UV-B irradiation also induces the degradation of the D1 reaction center protein. The rate of the D1 protein loss is slower than the inhibition of oxygen evolution and of the multiline signal but follows closely the loss of Signal II_{slow}, the Q_A⁻Fe²⁺ and the Fe³⁺ EPR signals, as well as the release of protein-bound manganese. It is concluded from the results that UV-B radiation affects photosystem II redox components at both the donor and acceptor side. The primary damage occurs at the water-oxidizing complex. Modification and/or inactivation of tyrosine-D, cytochrome *b*-559, and the Q_AFe²⁺ acceptor complex are subsequent events that coincide more closely with the UV-B-induced damage to the protein structure of the photosystem II reaction center.

Solar radiation exerts a multitude of effects on the photosynthetic apparatus. Beyond being the ultimate driving force of photosynthesis and its important regulatory factor, light is also a major source of stress to photosynthetic organisms. Light stress is induced both in the visible and in the ultraviolet spectral range of solar radiation. Inhibition of photosynthesis by high-intensity visible light, called photoinhibition, is now understood to a considerable amount at the molecular level; for recent reviews, see Aro et al. (1993), Barber and Andersson (1992), and Andersson and Styring (1991). Much less is known about the precise mechanism of damage caused by UV radiation. In this respect, the UV-B region (280–320 nm) of the solar spectrum is of special importance since the depletion of stratospheric ozone by man-made chemicals specifically enhances the flux of UV-B radiation on the surface of earth and in ecologically significant depths of the ocean (Stolarski et al., 1992; Kerr & McElroy, 1993; Smith et al., 1995).

UV-B radiation targets multiple sites in the photosynthetic apparatus, including photosystem II (PSII),¹ photosystem I (PSI), and the light-harvesting complex, but there is a consensus that PSII is the predominantly sensitive site of the UV-B attack [for a review, see Bornman (1986)].

PSII is a multifunctional pigment–protein complex in the thylakoid membrane that catalyzes the light-driven oxidation of water and the reduction of the plastoquinone pool [for recent reviews, see Andersson and Styring (1991) and Debus (1992)]. The reaction center of PSII consists of the heterodimer of the D1 and D2 proteins (Nanba & Satoh, 1987). The D1/D2 heterodimer binds or contains the redox cofactors of light-induced PSII electron transport: the primary electron donor chlorophyll (P₆₈₀), the primary electron acceptor pheophytin (Pheo), the tyrosine electron donors to P₆₈₀ (Tyr-Z and Tyr-D), and the quinone–iron electron acceptor complex consisting of the Q_A and Q_B quinone molecules and the non-heme iron. The catalytic manganese cluster of water oxidation is most likely also bound to the reaction center heterodimer [see Andersson and Styring (1991) and Debus (1992)].

[†] The work was supported by grants from NATO [OUTREACH-(LG.940992)5408], the Hungarian Granting Agency OTKA (T 017049), and the EU (Network Grant ERBCHRXCT940524).

^{*} Corresponding author: Imre Vass, Institute of Plant Biology, Biological Research Center, H-6701 Szeged, P.O. Box 521, Hungary. Telephone: 36-62-432-232. Fax: 36-62-433-434. E-mail: H419VAS@ELLA.HU.

[‡] Biological Research Center.

[§] University of Crete.

^{||} National Center for Scientific Research "Demokritos".

[®] Abstract published in *Advance ACS Abstracts*, June 15, 1996.

¹ Abbreviations: cyt *b*-559, cytochrome *b*-559; PSII, photosystem II; P₆₈₀, the reaction center chlorophyll of PSII; Q_A, the first quinone electron acceptor of PSII; Q_B, the second quinone electron acceptor of PSII; Pheo, the pheophytin electron acceptor of PSII; Tyr-Z, the immediate tyrosine electron donor of P₆₈₀; Tyr-D, the accessory tyrosine electron donor of P₆₈₀.

The harmful effects of UV-B radiation on the PSII function and structure are manifested as inhibition of electron transport (Jones & Kok, 1966a,b; Bornman et al., 1984; Tevini & Pfister, 1984; Renger et al., 1989; Melis et al., 1992; Hideg et al., 1993) and degradation of the D1 and D2 reaction center proteins (Greenberg et al., 1989a,b; Trebst & Depka, 1990; Melis et al., 1992; Friso et al., 1993, 1994; Barbato et al., 1995). However, the precise molecular targets of UV-B radiation in PSII are still controversial. A number of previous investigations tended to support the principal sensitivity of the PSII donor side, especially the water-oxidizing complex, with additional damage to the acceptor side components (Jones & Kok, 1966a,b; Bornman et al., 1984; Tevini & Pfister, 1984; Renger et al., 1989). Other studies suggested the quinone electron acceptors (Renger et al., 1986; Trebst & Depka, 1990) or the redox-active tyrosines, Tyr-Z in particular (Yerkes et al., 1990), as the primary site of UV-B action in PSII. The apparent conflict regarding the relative UV-B sensitivity of PSII redox components has not been resolved by more recent studies either. On the basis of the impaired photoreduction of Q_A and PQ, Melis et al. (1992) suggested that UV-B damage of the quinone electron acceptors is responsible for the loss of PSII electron transport. In contrast to this, Hideg et al. (1993) provided further support in favor of the water-oxidizing complex being the primary site of UV-B damage in PSII by using thermoluminescence measurements.

In the present work, we performed a thorough, comparative characterization of the UV-B effect on the redox components of PSII using low-temperature EPR spectroscopy in combination with chlorophyll fluorescence measurements and protein analysis. Our results demonstrate that the primary UV-B damage occurs at the electron transfer step between the Mn cluster of water oxidation and Tyr-Z⁺, with subsequent impairment of the quinone electron acceptors and the redox-active tyrosines.

MATERIALS AND METHODS

PSII membranes were isolated from spinach as described earlier (Vass et al., 1995) and stored at -80°C until use in 0.4 M sucrose, 5 mM MgCl_2 , 10 mM NaCl, and 40 mM Mes (pH 6.5) at 2–3 mg of Chl/mL. UV-B irradiation was performed by using a VL-215M (Vilber Lourmat) lamp giving an intensity of about $50\ \mu\text{Em}^{-2}\ \text{s}^{-1}$. The maximal emission from the lamp is at 312 nm, with an about 20 nm half-band width. PSII membranes, at 1000 μg of Chl/mL in a 1 mm layer, were illuminated in a Petri dish at 10 cm from the sample surface, with slow stirring on ice. The average UV-B dose which is effective in inactivating PSII was calculated by taking into account the absorption by the optically dense sample according to Rontó et al. (1989). The UV-B-irradiated PSII membranes were dark adapted for 10 min at room temperature before preparing the EPR samples.

Steady-state rates of oxygen evolution were measured polarographically at saturating light in the presence of 0.3 mM 2,5-dimethyl-*p*-benzoquinone as an exogenous electron acceptor.

X-Band low-temperature EPR spectra were recorded under nonsaturating conditions at a 9.42 GHz microwave frequency with a Bruker ESP 200D spectrometer equipped with an Oxford Instruments cryostat and temperature controller. Illumination of the EPR samples was performed in an

unsilvered dewar from an 860 W projector lamp through a heat-absorbing CuSO_4 filter at 77 K (in liquid nitrogen) or at 200 K (in acetone cooled by liquid nitrogen). Data acquisition and analysis was performed by home-made software.

The kinetic EPR measurements were carried out with a Bruker ER200D X-band spectrometer in a flat sample cell, at about 1.5 mg of Chl/mL as described earlier (Bakou & Ghanotakis, 1993). The saturating exciting flashes were provided by an EG&G xenon flash lamp system. The rise and decay of the photoinduced signal was followed by a DSP model 2824SA transient recorder/signal averager.

Light-induced changes in the chlorophyll fluorescence yield were measured by a PAM fluorimeter (Walz, Effeltrich, Germany). For data acquisition and analysis, the FIP software of Q_A Data (Turku, Finland) was used.

UV-B-induced changes in the protein structure of PSII were followed by SDS-PAGE on a 12 to 17% linear acrylamide gradient gel containing 6 M urea as described earlier (Friso et al., 1993). For detection of the D1 reaction center protein by immunoblotting, the resolved proteins were transferred to a nitrocellulose filter (Sartorius 45 μm) by electroblotting and identified by using a polyclonal antibody raised against the D1 protein (a kind gift of Dr. Roberto Barbato, Padova). The reaction was visualized by a colorimetric method as described earlier (Friso et al., 1993), and the immunodecorated blots were analyzed by a Biorad 1650 densitometer attached to a Hewlett-Packard integrator (HP 33941).

RESULTS

UV-B Effects on the Water-Oxidizing Complex

A putative target of UV-B radiation in PSII is the water-oxidizing complex (Jones & Kok, 1966a,b; Bornman et al., 1984; Tevini & Pfister, 1984; Renger et al., 1989; Hideg et al., 1993). We applied EPR spectroscopy and chlorophyll fluorescence measurements in order to clarify the site and extent of its damage by UV-B irradiation.

Variable Fluorescence. Light-induced reduction of Q_A by electrons extracted from the water-oxidizing complex results in an increase of chlorophyll fluorescence yield. The ratio of the variable fluorescence, i.e. the difference of the maximal, F_m , and the initial, F_o , fluorescence yields, relative to F_m (F_v/F_m) is considered to be proportional to the quantum yield of PSII for reducing Q_A (Dau, 1994). UV-B irradiation of PSII membranes markedly slows the light-induced rise of the fluorescence yield and decreases the F_m level, concomitant with a small increase in the initial F_o fluorescence yield (Figure 1). As a result of these changes, F_v/F_m decreases to about 70% of its original value after 30 min of irradiation and to 50% after 80 min of irradiation. Under the same conditions, the steady-state yield of oxygen evolution is decreased to 50 and 10% of the control activity after 30 and 80 min of UV-B treatment, respectively (see below, in Figure 9B). Since a slow rise of the variable fluorescence transient and its diminished F_m yield are characteristic features of donor side limitation of PSII (Dau, 1994), the occurrence of these phenomena in the UV-B-irradiated PSII membranes indicates the retardation of electron transfer from the water-oxidizing complex to Q_A .

S_2 -State Multiline Signal. Redox functioning of the water-oxidizing complex can be directly monitored by measuring

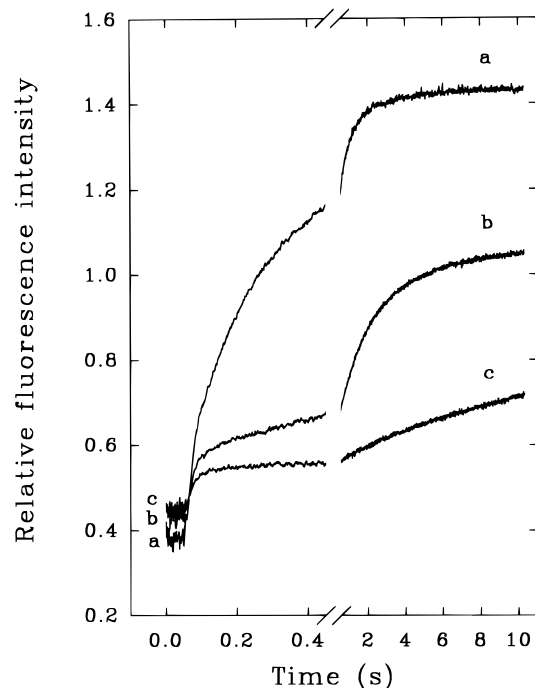


FIGURE 1: Effect of UV-B irradiation on the variable fluorescence transient of PSII membranes. The light-induced rise of chlorophyll *a* fluorescence was measured in nontreated control membranes (a) and after 30 (b) and 80 (c) min of UV-B irradiation. The data are shown on a split time scale, from 0 to 450 ms and from 0.45 to 10 s.

the so-called multiline EPR signal from the S_2 state (Dismukes & Siderer, 1981). The multiline signal is strongly decreased after 30 min of UV-B irradiation and is almost completely abolished after 80 min of irradiation (Figure 2). At the same time, there is no observable evolution of the $g = 4.1$ signal (not shown), which represents an alternative signal from the S_2 state (Casey & Sauer, 1984; Zimmermann & Rutherford, 1984; Dismukes, 1986). In our experiments, the multiline signal was induced by illumination at 200 K. At this temperature, the S_1 to S_2 transition takes place and the electron can be transferred to Q_A , but the Q_A to Q_B transition is inhibited. Thus, limited multiline signal formation in the UV-B-irradiated PSII membranes reports a lesion of electron transport somewhere between the water-oxidizing complex and Q_A .

Hexaquomanganese Signal. Inactivation of the water-oxidizing complex can lead to the release of the catalytic Mn ions from their binding site on the reaction center heterodimer [see Debus (1992)]. The released Mn can be detected by measuring the hexaquomanganese signal arising from the interaction of Mn with water. In the UV-B-irradiated PSII membranes, the loss of oxygen evolution and multiline signal formation is accompanied by the induction of the hexaquomanganese EPR signal (not shown). The signal increases gradually during the course of UV-B irradiation. However, after 80 min of irradiation, when multiline signal formation is hardly observed (Figure 2), only 30% of the total Mn is released as quantified by releasing all manganese by HCl (see below in Figure 9D).

UV-B Effects on the Redox-Active Tyrosines

Tyrosines absorb at around 280 nm in their reduced form and at around 310 nm in their oxidized radical form, as demonstrated for Tyr-Z (Diner & de Vitry, 1995; Dekker et

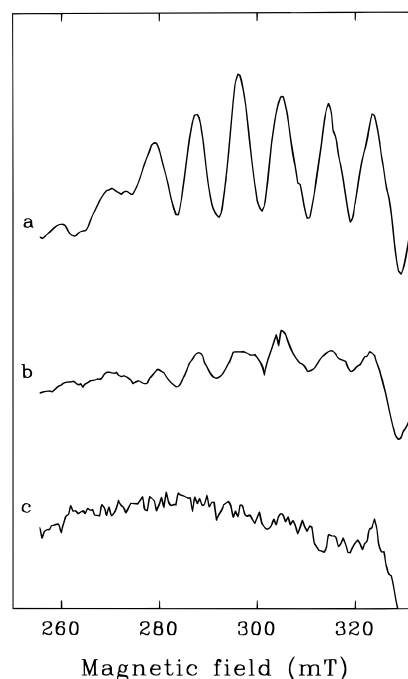


FIGURE 2: Effect of UV-B radiation on the multiline EPR signal of PSII membrane particles. The multiline signal was induced by 10 min of illumination at 200 K in samples which had been exposed to UV-B irradiation for 0 (a), 30 (b), and 80 min (c). The six-line EPR signal from free manganese was eliminated by addition of 3 mM EDTA. The spectra are shown as light minus dark difference spectra. The EPR conditions were as follows: temperature = 10 K, microwave power = 20 mW, and modulation amplitude = 2.5 mT.

al., 1984; Gerken et al., 1988). On the basis of these absorption characteristics, both Tyr-Z and Tyr-D have been considered targets of UV-B radiation (Yerkes et al., 1990). In order to follow UV-B-induced changes in the redox function of Tyr-D and Tyr-Z, we measured the EPR signals arising from the oxidized radical form of these residues.

Signal II_{slow} . Tyr- D^+ is remarkably stable in the dark and gives rise to the EPR Signal II_{slow} (Babcock & Sauer, 1973). As a consequence of UV-B irradiation, the amplitude of Signal II_{slow} gradually decreases with increasing irradiation time. However, its loss is less pronounced than that of the multiline signal, and about 50% of the original Signal II_{slow} can still be detected after 80 min of irradiation (Figure 3). This observation implies that Tyr-D or its environment is damaged by UV-B but also that Tyr-D is more resistant against the UV-B attack than the water-oxidizing complex.

Signal II_{fast} . In normally functioning PSII, the lifetime of Tyr- Z^+ is so short that the EPR signal from this species, called Signal $II_{very fast}$, can only be observed with time-resolved measurements in the microsecond range (Hoganson & Babcock, 1988). When electron transport from the water-oxidizing complex is inhibited, the lifetime of Tyr- Z^+ increases to the millisecond time range and the so-called Signal II_{fast} appears, which has the same shape as Signal II_{slow} (Blankenship et al., 1975). We applied time-resolved EPR measurements to monitor the effect of UV-B irradiation on the transient formation of Signal II_{fast} . In the nonirradiated control samples, Signal II_{fast} is almost completely absent and can only be seen after inactivating the water-oxidizing complex by Tris washing (Figure 4). The small signal that is observed without Tris treatment most likely arises from PSII centers whose donor side lost integrity during isolation.

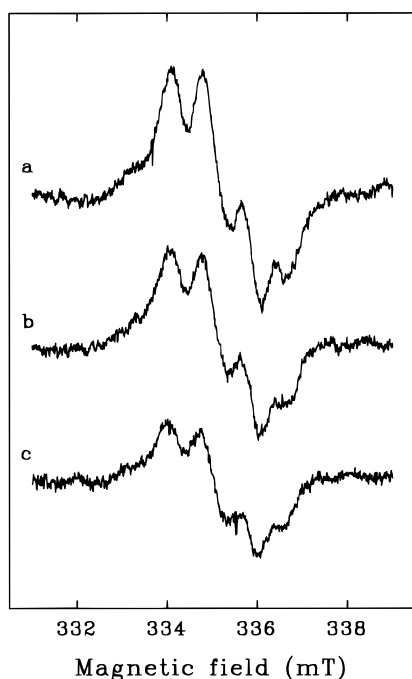


FIGURE 3: Effect of UV-B irradiation on Signal II_{slow} of PSII membrane particles. The dark stable Signal II_{slow} was measured in samples which had been irradiated with UV-B for 0 (a), 30 (b), and 80 min (c). Before the EPR measurements, all samples were illuminated with visible light for 1 min to oxidize Tyr-D uniformly. The EPR conditions were as follows: temperature = 10 K, microwave power = 200 nW, and modulation amplitude = 0.32 mT.

Importantly, in the UV-B-irradiated PSII membranes, Signal II_{fast} is induced even without the inactivating Tris treatment, and its amplitude is enhanced during the course of irradiation (Figure 4). In contrast, the full amplitude of Signal II_{fast}, which is observed after Tris treatment of the irradiated samples, decreases. These observations are consistent with the inhibition of electron donation from the water-oxidizing complex to Tyr-Z⁺ in the irradiated samples and also with the partial impairment of Tyr-Z redox functioning.

UV-B Effects on the Quinone–Iron Acceptor Complex

The series of one-electron transfer steps within the PSII complex is interfaced to the two-electron reduction of plastoquinone by the so-called two-electron gate, which consisted of Q_A and Q_B in close interaction with the non-heme iron [see Diner et al. (1991)]. Due to their absorption in the UV-B spectral range, the quinone electron acceptors are frequently considered the main targets of UV-B radiation in PSII (Greenberg et al., 1989a,b; Trebst & Depka, 1990; Melis et al., 1992). In order to study the extent of UV-B-induced damage to the function of the quinone–iron acceptor complex, we applied EPR and chlorophyll fluorescence measurements.

The Q_A^{•−}Fe²⁺ Signal. The interaction of Q_A^{•−} and Fe²⁺ gives rise to an EPR signal in the $g = 1.8$ – 1.9 range, providing a useful marker of Q_A reduction (Nugent et al., 1981; Rutherford & Zimmermann, 1984). This signal is generally small but can be enhanced significantly by the addition of formate (Vermaas & Rutherford, 1984). Q_A reduction in our experiments was induced by illumination at 77 K. At this temperature, the primary charge separation and electron transfer to Q_A is active, but the S₁ to S₂ transition

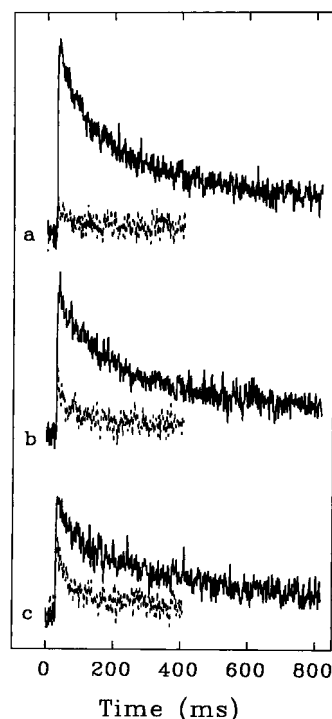


FIGURE 4: Effect of UV-B radiation on the flash-induced formation of Signal II_{fast}. The kinetic traces were measured at the low-field peak position of Signal II in nontreated controls (a) and after 30 (b) and 80 (c) min of UV-B irradiation. The dashed and solid curves were measured without further treatment and after Tris washing of the samples, respectively. The PSII membranes contained an equimolar (3 mM) mixture of ferricyanide and ferrocyanide as an acceptor system. Each curve is the average of 200 traces measured with a repetition rate of 0.3 Hz. The EPR conditions were as follows: temperature = 293 K, microwave power = 20 mW, modulation amplitude = 0.4 mT, and time constant = 1 ms.

is inhibited and alternative electron donors, such as cyt b-559 and the accessory chlorophylls, act as donors to Tyr-Z⁺ and/or P₆₈₀⁺ (Miller & Brudvig, 1991; Buser et al., 1992). The measurements in Figure 5 show that light-induced formation of the Q_A^{•−}Fe²⁺ signal is suppressed in the UV-B-irradiated PSII membranes. It is also clear that the inhibition of the Q_A^{•−}Fe²⁺ signal is less pronounced than that observed for the multiline signal, since after 80 min of irradiation about half of the original Q_A^{•−}Fe²⁺ signal can still be induced (Figure 5), in contrast to the almost complete loss of the multiline signal (Figure 2).

To clarify whether the loss of the Q_A^{•−}Fe²⁺ signal was due to a direct UV-B effect on the quinone–iron complex, or influenced by the impairment of Tyr-Z or of the alternative donors which function at 77 K, Q_A was also reduced chemically by dithionite. The size of the Q_A^{•−}Fe²⁺ signal in the dithionite-reduced samples is somewhat larger than in the 77 K illuminated samples (not shown). However, the effect of UV-B irradiation on the decrease of the signal size is similar in both cases (see Figure 9A below). These observations are consistent with the function of the Q_AFe²⁺ complex being affected by UV-B radiation, but it is also obvious that this site is less sensitive than the water-oxidizing complex.

Fe³⁺ Signal. Since the Q_A^{•−}Fe²⁺ signal arises from the interaction of Q_A^{•−} and Fe²⁺ (Nugent et al., 1981; Rutherford & Zimmermann, 1984), its loss upon UV-B irradiation can be induced by damage either of Q_A^{•−} or of the iron. This uncertainty can be clarified by verifying directly the presence

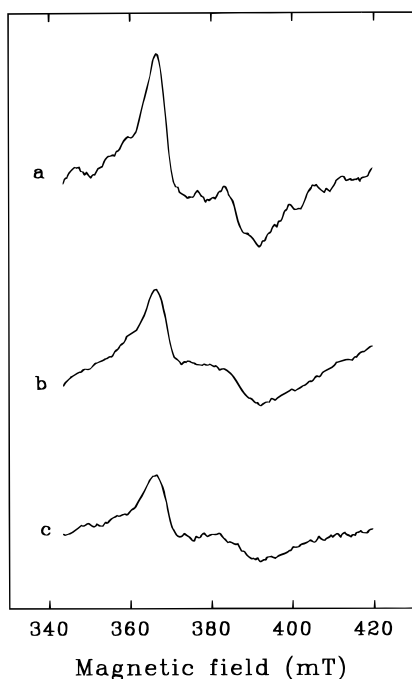


FIGURE 5: Effect of UV-B radiation on the $Q_A^-Fe^{2+}$ EPR signal of PSII membrane particles. The reduction of Q_A was induced by 10 min of illumination at 77 K in samples which had been exposed to UV-B irradiation for 0 (a), 30 (b), and 80 min (c) and contained 3 mM EDTA to remove free manganese. Formate (100 mM) was added after the UV-B irradiation in order to enhance the $Q_A^-Fe^{2+}$ signal. The curves shown are light minus dark difference spectra. The EPR conditions were as follows: temperature = 4.2 K, microwave power = 32 mW, and modulation amplitude = 3.2 mT.

and redox activity of the non-heme iron by measuring the EPR signal arising from its oxidized (Fe^{3+}) state. In our experiments, the iron was oxidized in the dark by potassium ferricyanide, and the oxidized minus initially reduced EPR spectra were obtained in the control and irradiated samples (Figure 6). The Fe^{3+} signal in the nonirradiated control is characterized by peaks at around $g = 8$ and 5.6 (Petrouleas & Diner, 1986). UV-B irradiation has a twofold effect on the Fe^{3+} EPR spectra. On the one hand, the $g = 8$ and 5.6 peaks are gradually decreased. On the other hand, a new signal appears at around $g = 4.26$ with a clearly resolved double peak (Figure 6). Illumination of the oxidized samples by visible light at 200 K reduces the $g = 8$ and 5.6 signals, but the $g = 4.26$ signal is not affected (not shown). It is likely that the latter signal results from a modified environment of the iron in damaged centers (see also Discussion). The extent by which the $g = 8$ and 5.6 signals of Fe^{3+} are decreased as a consequence of UV-B irradiation is similar or even smaller than the decrease of the $Q_A^-Fe^{2+}$ signal, i.e. 60% of the original Fe^{3+} remains after 80 min of irradiation (Figure 6; see also Figure 9A below).

UV-B Effects on Cytochrome *b*-559 and on the D1 Protein

The redox state of cyt *b*-559 is a sensitive indicator of the integrity of PSII. In intact centers, cyt *b*-559 is mostly in the high-potential form that stays reduced in the dark and can be oxidized by illumination at low temperatures (77 K) (De Paula et al., 1988). In contrast, in centers with a modified or damaged structure of PSII, cyt *b*-559 is generally converted to the low-potential form which is easily oxidized in the dark (Thompson et al., 1989). In order to check if

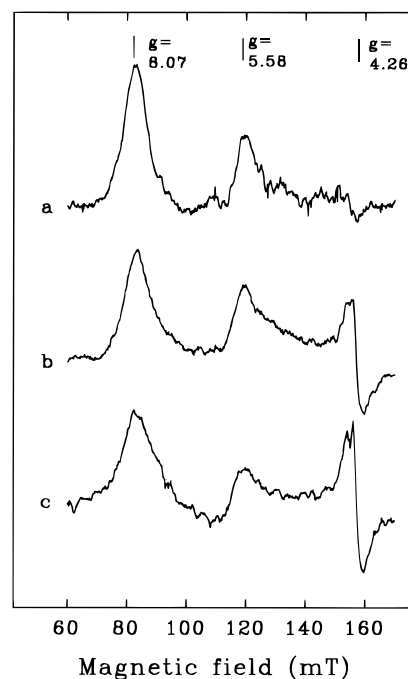


FIGURE 6: Effect of UV-B radiation on the Fe^{3+} EPR signal of PSII membrane particles. The oxidation of the non-heme iron from its Fe^{2+} to the Fe^{3+} form was induced by incubating the samples with 5 mM potassium ferricyanide for 30 min in the dark at room temperature. The samples had previously been irradiated with UV-B for 0 (a), 31 (b), and 80 min (c). The curves shown are the oxidized minus initially reduced difference spectra obtained after and before the incubation with FeCy, respectively. The EPR conditions were as follows: temperature = 4.2 K, microwave power = 8 mW, and modulation amplitude = 1.6 mT.

irradiation by UV-B has any direct or indirect effect on the redox state of cyt *b*-559, the EPR signals arising from the dark-oxidized and photo-oxidized forms of cyt *b*-559 have been measured. In the nonirradiated control samples, the EPR signal at $g = 2.94$ (Figure 7, solid curve a) shows the presence of dark-oxidized cyt *b*-559. Illumination of these samples at 77 K results in an increase of the EPR signal at $g = 3.06$ due to oxidation of the population of cyt *b*-559 which stayed in the reduced form in the dark (Figure 7, dotted curve a). In the UV-B-irradiated samples, the size of the $g = 2.94$ signal increases and after 80 min of irradiation is almost doubled relative to what appears in the nonirradiated control (Figure 7, solid line c). Concomitantly with this effect, the light-induced signal at $g = 3.06$ gradually decreases, and therefore, the total amount of EPR detectable cyt *b*-559 appears to remain stable. These observations indicate that UV-B increases the amount of dark-oxidizable cyt *b*-559 population, appearing at $g = 2.94$, at the expense of the light-oxidizable form, giving rise to the EPR signal at $g = 3.06$.

The amount of the D1 reaction center protein is also decreased as a consequence of UV-B irradiation of the PSII membranes as detected by immunoblotting (Figure 8). The extent of D1 protein loss is smaller than that of oxygen evolution and reaches about 60% of its value in the nonirradiated control after 80 min of irradiation (see below in Figure 9D).

DISCUSSION

UV-B radiation is a well-known cause of damage to the function and structure of PSII. Previous studies have

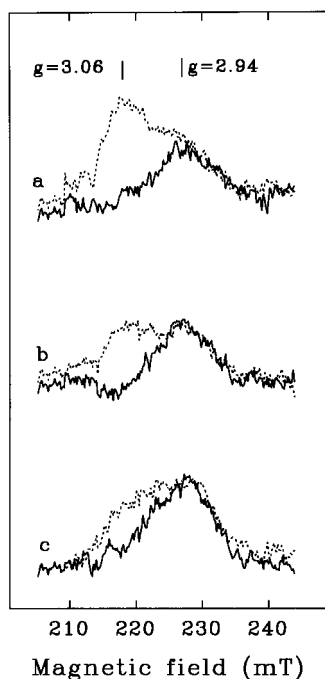


FIGURE 7: Effect of UV-B irradiation on cyt b-559 of PSII membrane particles. The samples had been irradiated with UV-B for 0 (a), 31 (b), and 80 min (c), and the EPR spectra were measured either on dark-adapted samples (solid curves) or after 10 min of illumination at 77 K. The EPR conditions were as follows: temperature = 4.2 K, microwave power = 6.3 mW, and modulation amplitude = 1.25 mT.

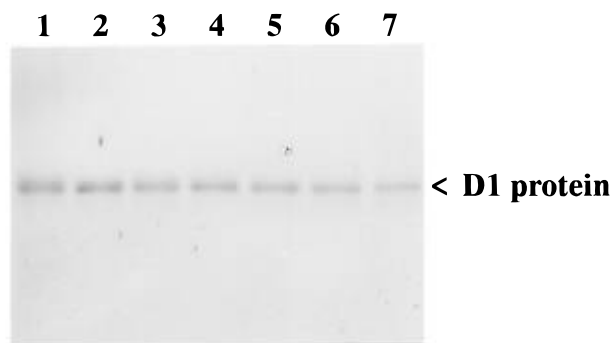


FIGURE 8: Immunodetection of D1 protein in UV-B-irradiated PSII membrane particles. Samples were kept in the dark for 80 min (lane 1) or irradiated with UV-B for 10 (lane 2), 20 (lane 3), 30 (lane 4), 45 (lane 5), 60 (lane 6), and 80 min (lane 7).

revealed various molecular targets within PSII: the water-oxidizing complex (Jones & Kok, 1966a,b; Bornman et al., 1984; Tevini & Pfister, 1984; Renger et al., 1989; Hideg et al., 1993), the quinone electron acceptors (Renger et al., 1986; Trebst & Depka, 1990; Melis et al., 1992), and the redox-active tyrosines (Yerkes et al., 1990). However, no agreement has been reached concerning the relative UV-B sensitivity and the significance of these target molecules in the overall UV-B effect. Our results show that, although UV-B radiation affects all of the previously suggested action sites in PSII electron transport, the extent of their damage is clearly different.

UV-B Effects on the $Q_A\text{Fe}^{2+}Q_B$ Acceptor Complex. On the basis of their absorption in the UV-B region, the plastoquinone electron acceptors of PSII have repeatedly been suggested as primary targets of UV-B radiation in PSII (Greenberg et al., 1989a,b; Trebst & Depka, 1990; Melis et al., 1992). Indeed, we observed that the light-induced EPR

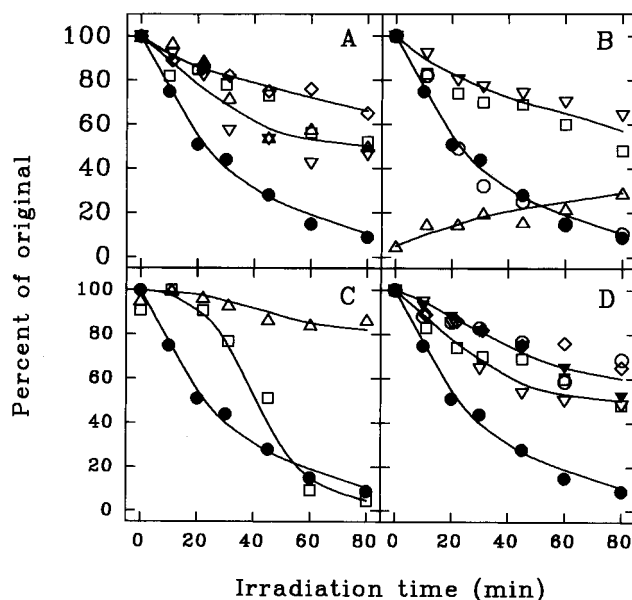


FIGURE 9: Time course of PSII activity loss during UV-B irradiation. The EPR signals, variable fluorescence, and the D1 protein were measured as described in Materials and Methods as well as in Figures 1–8 and plotted as a function of UV-B irradiation time in percentage of their value in the nonirradiated controls: (A) the $Q_A\text{Fe}^{2+}$ signal induced by illumination at 77 K (Δ), the $Q_A\text{Fe}^{2+}$ signal induced by incubation with 50 mM sodium dithionite (∇), the $g = 8.06$ peak of the Fe^{3+} signal (\diamond), F_v/F_m (\square), and steady-state oxygen evolution (\bullet); (B) steady-state oxygen evolution (\bullet), multiline signal (\circ), Signal II_{slow} (\square), Signal II_{fast} (Δ), and Signal II_{fast} after Tris washing (∇); (C) the total amount of cyt b-559 obtained after illumination at 77 K (Δ), the light inducible part of cyt b-559 obtained as the difference of 77 K illuminated and dark spectra (\square), and steady-state oxygen evolution (\bullet); (D) D1 protein (\blacktriangledown), the amount of membrane-bound Mn, obtained as the difference of the full amount of Mn that can be released by HCl treatment and the Mn that is released as a consequence of UV-B irradiation (\circ), Signal II_{slow} (\square), the $Q_A\text{Fe}^{2+}$ signal (∇), and steady-state oxygen evolution (\bullet).

signal arising from the interaction of Q_A^- and Fe^{2+} is decreased as a consequence of UV-B irradiation (Figure 5). The decrease of the light-induced $Q_A\text{Fe}^{2+}$ EPR signal may not necessarily reflect destruction of Q_A itself. Inhibition of electron transfer from the PSII donor side to Q_A , modification or damage of the non-heme iron, as well as alteration of the protein environment around the Q_A site could also diminish the $Q_A\text{Fe}^{2+}$ signal.

The first alternative is ruled out by showing that the induction of the $Q_A\text{Fe}^{2+}$ signal by dark, chemical reduction using dithionite is inhibited in the irradiated samples to the same extent as in the light-induced $Q_A\text{Fe}^{2+}$ signal (Figure 9A). Thus, electron transport from the donor side of PSII is not limiting Q_A reduction during 77 K illumination.

The second alternative concerns the modification or loss of the non-heme iron. The $Q_A\text{Fe}^{2+}$ signal was recorded in the presence of formate, which binds at or in the vicinity of the non-heme iron (Diner & Petrouleas, 1990). A UV-induced modification of the binding affinity of formate could explain the loss of the $Q_A\text{Fe}^{2+}$ signal. As, however, the Fe^{3+} EPR signals are very sensitive to changes in the environment of the iron (Deligiannakis et al., 1994, and references therein) and the Fe^{3+} signal remains detectable to a large percentage (somewhat larger than the $Q_A\text{Fe}^{2+}$ signal), one might claim that the primary cause for the loss

of the $Q_A^-Fe^{2+}$ signal is damage occurring at Q_A or its immediate environment.

The gradual loss of the Fe^{3+} signal at $g = 8.06$ and 5.6 could be due to a number of reasons, e.g. increase of the redox potential, modification of the protein environment around the iron, or loss of the iron from its binding site. The second alternative is supported by the induction of a signal at $g = 4.26$ with resolved structure in the irradiated samples (Figure 6). A very similar signal attributed to the non-heme iron has been observed in PSII membranes treated with various carboxylate anions (Deligiannakis et al., 1994). The lack of light sensitivity of the $g = 4.26$ signal in the present case could be explained by the parallel loss of Q_A^- formation. The similarity of the signal observed in the UV-B-irradiated and carboxylate anion-treated samples does not necessarily imply identity of the iron ligands in the two cases. It generally implies a ligand geometry imposing a weak field with large rhombicity (small D , large E/D) (Deligiannakis et al., 1994). Despite its apparently large intensity, the $g = 4.26$ signal probably represents a small fraction of centers (Deligiannakis et al., 1994). It is likely that the $g = 4.26$ signal arises from partially damaged centers in which the protein environment around the iron is modified (but see further discussion below).

The electrons from Q_A are accepted by the second quinone, Q_B , whose function may also be affected by UV-B radiation. This question was approached by measuring light-induced changes in the chlorophyll fluorescence yield. Preferential damage of Q_B or the plastoquinones in the pool would inhibit the reoxidation of Q_A^- which in turn would accelerate the rise of variable fluorescence. This expectation is just opposite to the slowing of the fluorescence yield increase observed in the UV-B-irradiated PSII membranes (Figure 1). Thus, a significantly faster damage of Q_B (and PQ) than of Q_A is unlikely. This is further corroborated by the lack of change in the relaxation kinetics of flash-induced fluorescence yield (not shown), indicating that the rate of electron transfer between Q_A and Q_B is not seriously affected. Secondary damage of the Q_B binding niche may, however, occur as shown by the decreased binding affinity of DCMU and atrazine and also of PQ at the Q_B site as a consequence of UV-B irradiation of thylakoids (Hideg et al., 1993; Renger et al., 1986, 1989). It is also of note that the F_v/F_m fluorescence parameter, which is proportional to the quantum yield of PSII for Q_A reduction, declines much slower than oxygen evolution and follows closely the decay course of the $Q_A^-Fe^{2+}$ EPR signal (Figure 9A). This indicates that during prolonged illumination Q_A^- can be slowly accumulated even in those PSII centers in which the function of the water-oxidizing complex is largely inhibited by the UV-B effect.

UV-B Effects on the Redox-Active Tyrosines. Tyrosines absorb at around 280 nm in the reduced form and at around 300 nm in the oxidized radical form and thus can be direct targets of UV-B radiation. UV-B-induced destruction of tyrosines has been observed both in the free amino acid form and in proteins (Vladimirov et al., 1970). The decline of Signal II_{slow} and Signal II_{fast} in Tris-treated samples indicates that both Tyr-D and Tyr-Z are damaged by UV-B irradiation (Figures 3 and 4). This, in agreement with previous results of Yerkes et al. (1990), shows that the redox-active tyrosine residues of the PSII reaction center are prone to UV-B attack. However, we also demonstrate that Tyr-D and Tyr-Z are not

the primary targets of UV-B in the PSII complex since the loss of their redox activity is slower than the inhibition of oxygen evolution (Figure 8B).

As tyrosines are expected to have more efficient absorption in the UV-B range in the oxidized than in the reduced form, one would expect more extensive damage to Tyr-D⁺ than to Tyr-Z, which would normally be in the reduced state. The almost parallel loss of Tyr-Z⁺ and Tyr-D⁺ formation in our experiments can be explained by the stabilization of Tyr-Z⁺ due to UV-B impairment of electron transfer from the Mn cluster. Since the relatively intense UV-B illumination applied in our experiments can partially drive PSII electron transport (not shown), it may accumulate the oxidized radical form of Tyr-Z in the centers with the impaired Mn cluster. The Tyr-Z⁺ population thus formed can be destroyed with similar efficiency as Tyr-D⁺. Alternatively, the similar extent of UV-B damage to Tyr-Z⁺ and Tyr-D⁺ may indicate that the redox activity of Tyr-Z and Tyr-D is lost due to indirect damage, mediated by the protein matrix, rather than to direct destruction of the tyrosines due their UV-B absorption.

UV-B Effects on the Water-Oxidizing Complex. Inhibition of steady-state oxygen evolution, which reflects the loss of electron transport through PSII, is followed closely by the decline of the S₂-state multiline signal (Figure 9B). Charge stabilization in the S₂ state, the prerequisite of multiline signal formation, requires uninterrupted electron transport from the water-oxidizing complex to Q_A . Light-induced reduction of Q_A at 77 K by alternative electron donors, such as cyt b-559 or the accessory chlorophylls, is impaired to a significantly lesser extent (about 50% loss after 80 min of irradiation) than the multiline signal (about 90% loss after 80 min of irradiation) (Figure 9B). Thus, damage of Q_A or of the electron transport from P₆₈₀ to Q_A cannot be the primary cause for the inhibition of S₂ state formation.

Electron donation from water to P₆₈₀ is mediated by Tyr-Z, which is now believed to be closely associated with the water-oxidizing complex (Gilchrist et al., 1995; Babcock, 1995). The induction of Signal II_{fast} in the UV-B-irradiated samples (Figures 4 and 9B) shows that in part of the centers the stability of Tyr-Z⁺ is increased to the millisecond time range which is characteristic for the interruption of electron donation from the water-oxidizing complex to Tyr-Z⁺ (Bakou & Ghanotakis, 1993; Blankenship et al., 1986). This observation demonstrates the existence of PSII centers in which the Mn cluster is impaired but Tyr-Z and Q_A are still functional. Since the S₂-state multiline formation and oxygen evolution is impaired much faster than the redox function of Q_A and Tyr-Z, it is reasonable to conclude that the water-oxidizing complex is the most UV-B sensitive component of PSII.

The predominant damage of the water-oxidizing complex by UV-B is corroborated by the changes observed in the variable chlorophyll fluorescence transients, i.e. slowed fluorescence rise and the concomitant reduction of the F_m level (Figure 1). These characteristics are typical of retarded electron donation from the site of water oxidation to Q_A (Dau, 1994).

UV-B Effects on cyt b-559. The redox state of cyt b-559 strongly depends on the integrity of the PSII complex. In intact PSII membranes, the reduced high-potential form is the dominant species, which is easily converted to the auto-oxidizable low-potential form by different treatments, e.g. photoinhibition by visible light (Styring et al., 1990). We

observed similar changes as a consequence of UV-B irradiation. The amount of the dark-oxidized cyt b-559, giving rise to an EPR signal at $g = 2.94$, gradually increases, whereas the light inducible oxidation of the dark-reduced form decreases during the course of UV-B irradiation. In contrast, the total amount of dark- plus light-oxidizable cyt b-559 decreases only to a small extent even after 80 min of irradiation. In intact membranes, the high-potential form of cyt b-559 is mainly in the reduced state in the dark and can be photo-oxidized by low-temperature illumination (De Paula et al., 1988), whereas the low-potential form, which is usually observed in damaged PSII centers, is easily auto-oxidized in darkness (Thompson et al., 1989). Thus, our results may indicate that the high-potential population of cyt b-559 is converted to the low-potential form as a consequence of UV-B radiation, but cyt b-559 is rather resistant to UV-B irradiation in the low-potential form. The loss of light-induced cyt b-559 oxidation shows some correlation with the loss of oxygen evolution (Figure 9C). Consequently, the potential shift of cyt b-559 may be caused by a structural change in the PSII complex that is induced by the inactivation of the water-oxidizing complex.

UV-B Effects on the D1 Protein. UV-B-induced degradation of the D1 reaction center protein is a well-known phenomenon. However, the correlation of this effect with the inhibition of PSII redox components has not been studied in detail. The observation that D1 protein degradation occurs slower than the inhibition of oxygen evolution (Figure 9D) agrees with previous findings (Trebst & Depka, 1990; Friso et al., 1993). In addition, we also show that the release of protein-bound manganese, the loss of Tyr-D⁺, and the $Q_A^-Fe^{2+}$ and the Fe^{3+} ($g = 8$ and 5.6) EPR signals are closely correlated with the degradation of D1. As summarized in Figure 9D, the amount of membrane-bound manganese follows very closely the course of D1 protein degradation. This situation, which is very similar to that observed during photoinhibition by visible light (Virgin et al., 1988), shows that manganese release is not a direct consequence of UV-B inactivation of the water-oxidizing complex; rather, it is caused by losing the D1 protein and the integrity of the PSII complex. It is also interesting to note that the losses of the $Q_A^-Fe^{2+}$ and of the Fe^{3+} ($g = 8$ and 5.6) EPR signals show courses similar to that of the D1 protein (Figure 9D). This might indicate that the redox activity of Q_A and of the non-heme iron is lost due to a structural change of the PSII reaction center. UV-B-induced damage of the D1 protein, which provides binding ligands to the non-heme iron (Trebst, 1986; Michel & Deisenhofer, 1986), may induce a change in its protein environment and redox properties. This idea is in agreement with the observation of the light-insensitive $g = 4.26$ Fe^{3+} species, which could be assigned to centers in which the D1 protein is damaged or degraded.

Mechanistic Aspects of the UV-B Effect in PSII. UV-B-induced damage of PSII seems to have two main phases. In the first phase, electron transfer from the Mn cluster of water oxidation to Tyr-Z⁺ is impaired, but the tyrosine donors and the quinone-iron acceptor complex retain their function. In the second phase, the PSII centers are completely inactivated, including Tyr-Z, Tyr-D, the $Q_A^-Fe^{2+}$ complex, the D1 protein, and release of the protein-bound Mn. The loss of oxygen evolution and of the multiline signal gives a straight line when the natural logarithm of the relative activity is plotted

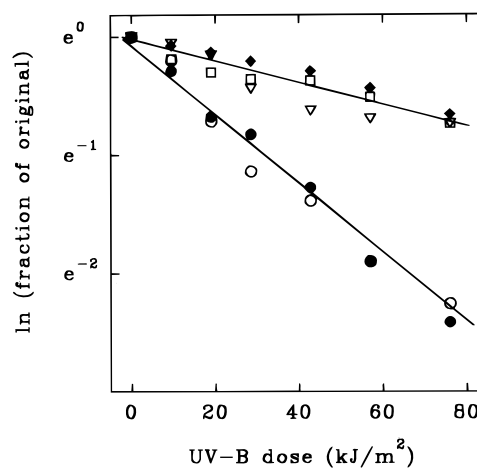


FIGURE 10: Semilogarithmic representation of the loss of various parameters of PSII activity during the course of UV-B irradiation. The measurements were performed as in Figures 1–8, and the natural logarithm of the proportion of the activity parameters relative to their original values is plotted as a function of the average UV-B dose, calculated as described in Materials and Methods: steady-state oxygen evolution (●), multiline signal (○), Signal II_{slow} (□), $Q_A^-Fe^{2+}$ (▽), and D1 protein (◆).

as a function of the irradiating dose (Figure 10). The loss of the $Q_A^-Fe^{2+}$ signal, Signal II_{slow}, Signal II_{fast}, and the D1 protein signal falls on another line with a smaller slope. According to the basic laws of radiobiology, this behavior indicates that inactivation of the given function is initiated by one hit of a single target (Tevini, 1993; Harm, 1980). The slope of the line is defined as the cross section of inactivation, i.e. the surface shown by the target to a single incident photon in the inactivating event. The inactivation cross section of oxygen evolution is 12.2 m²/mol of photon, whereas the cross section of inactivating the $Q_A^-Fe^{2+}$ complex, the redox-active tyrosines, and the D1 protein is only 3.7 m²/mol of photon. It is difficult to draw definite conclusions from the absolute cross section values, since it cannot be easily quantified what is the proportion of the UV-B quanta that is absorbed by the target molecule(s) in the PSII reaction center and by the other (protein and lipid constituents) of the thylakoid membrane. However, the 5-fold difference between the inactivation cross sections demonstrates that the UV-B sensitivity of the water-oxidizing complex is distinctly higher than those of the $Q_A^-Fe^{2+}$ complex, the redox-active tyrosines, and the D1 protein.

The mechanisms by which the PSII redox components are impaired by UV-B are not completely clear. In the case of the quinone acceptors and tyrosine donors, a direct destruction of the molecules could occur. However, the possibility that the redox function of these components is impaired due to damage of their protein environment cannot be excluded as indicated by the very similar inactivation cross sections of these components and of the D1 protein.

Damage or alteration of the protein binding environment of the catalytic Mn cluster is also the most likely scenario for inactivation of the water-oxidizing function, since the Mn ions themselves are not expected to be modified by UV-B. A direct UV-B hit of the manganese-ligating amino acid residue(s) is possible, but not very likely since the most UV-sensitive residues are the aromatic tyrosine, phenylalanine, tryptophane, as well as cysteine (Vladimirov et al., 1970), whereas Mn is expected to be ligated by histidines, aspartates, or glutamates [see Debus (1992)] which have not been shown

to be directly damaged by UV-B. Thus, it is more likely that UV-B radiation induces the alteration of the protein environment around the manganese cluster in more indirect ways without causing a prompt manganese release.

A possible mechanism of inactivation of the Mn site could be related to the specific structure of the 33 kDa water-soluble protein subunit of the water-oxidizing complex, which is retained in the UV-B-irradiated PSII membranes (not shown). The 33 kDa protein is expected to maintain the functional conformation of the Mn cluster (Miyao & Murata, 1984; Ono & Inoue, 1984; Vass et al., 1992) and unique among the PSII subunits in the sense that its proper conformation is likely to be stabilized by a disulfide bridge (Tanada & Wada, 1988; Irrgang et al., 1992). Since disulfide bridges can be split easily by UV-B radiation (Creed, 1984), this effect may lead to the inactivation of the catalytic Mn cluster.

The protein environment in the vicinity of the Mn cluster could also be damaged by reactive free radical species. It appears that free radicals, dominantly hydroxyl radicals, are formed in UV-B-irradiated PSII preparations (Hideg & Vass, 1995). The mechanism of this radical production in PSII is not fully understood yet, but one possibility is that they arise from the decomposition of H_2O_2 by UV-B as observed in model reactions (Czapski, 1984). Hydrogen peroxide has been suggested to appear as an intermediate during water oxidation (Renger, 1978; Wydrzynski et al., 1989). Thus, UV-B-induced decomposition of H_2O_2 could produce highly reactive hydroxyl radicals within the water-oxidizing complex and promote extensive damage to the protein environment.

CONCLUDING REMARKS

Our results show that UV-B radiation has multiple action sites in isolated PSII membranes. Among these sites, the water-oxidizing complex appears to be the most sensitive. The quinone-iron electron acceptor complex and the redox-active tyrosine donors are also affected by UV-B, but their UV-B sensitivity is about 5 times smaller than that of the water-oxidizing complex. Although it is not straightforward to extend the present EPR studies to intact photosynthetic systems, and to natural illumination conditions under which plants are exposed to the whole range of the solar spectrum reaching the earth, it is likely that the water-oxidizing complex is the primary action site of UV-B also *in vivo*. This view is corroborated by the markedly slowed and diminished rise of variable chlorophyll fluorescence yield, a fingerprint of inhibited electron transport from the water-oxidizing complex, that can be observed not only in PSII membrane particles but also in thylakoids (Bornman et al., 1984) and intact leaves (Bornman & Vogelmann, 1991).

ACKNOWLEDGMENT

We appreciate the help of Dr. Éva Hideg in preparing the UV-B-irradiated samples.

REFERENCES

Amesz, J. (1977) in *Encyclopedia of Plant Physiology*, Vol. 5 (Trebst, A., & Avron, M., Eds.) pp 238–246, Springer-Verlag, Berlin.

Andersson, B., & Styring, S. (1991) *Curr. Top. Bioenerg.* 16, 1–81.

Aro, E.-M., Virgin, I., & Andersson, B. (1993) *Biochim. Biophys. Acta* 1143, 113–134.

Babcock, G. T. (1995) in *Photosynthesis: from Light to Biosphere* (Mathis, P., Ed.) Vol. II, pp 209–215, Kluwer, Dordrecht.

Babcock, G. T., & Sauer, K. (1973) *Biochim. Biophys. Acta* 325, 483–503.

Bakou, A., & Ghanotakis, D. F. (1993) *Biochim. Biophys. Acta* 1141, 303–308.

Barbato, R., Frizzo, A., Friso, G., Rigoni, F., & Giacometti, G. M. (1995) *Eur. J. Biochem.* 227, 723–729.

Barber, J., & Andersson, B. (1992) *Trends Biochem. Sci.* 17, 61–66.

Blankenship, R. E., Babcock, G. T., Warden, J. T., & Sauer, K. (1975) *FEBS Lett.* 51, 287–293.

Bornman, J. F. (1986) *Photobiochem. Photobiophys.* 11, 9–17.

Bornman, J. F., Björn, L. O., & Akerlund, H.-E. (1984) *Photobiochem. Photobiophys.* 8, 305–313.

Brudvig, G. W. (1988) in *Metal Clusters in Biology* (Que, L., Ed.) American Chemical Society, Washington, DC.

Buser, C. A., Diner, B. A., & Brudvig, G. W. (1992) *Biochemistry* 31, 11449–11459.

Casey, J. L., & Sauer, K. (1984) *Biophys. J.*, 217a.

Creed, D. (1984) *Photochem. Photobiol.* 39, 577–583.

Czapski, G. (1984) *Methods Enzymol.* 105, pp 209–215.

Dau, H. (1994) *Photochem. Photobiol.* 60, 1–23.

De Paula, J. C., Innes, J. B., & Brudvig, G. W. (1988) *Biochemistry* 27, 8114–8120.

Debus, R. J. (1992) *Biochim. Biophys. Acta* 1102, 269–352.

Dekker, J. P., van Gorkom, H. J., Brok, M., & Ouwehand, L. (1984) *Biochim. Biophys. Acta* 764, 301–309.

Deligiannakis, Y., Petrouleas, V., & Diner, B. A. (1994) *Biochim. Biophys. Acta* 1188, 260–270.

Diner, B. A., & Petrouleas, V. (1990) *Biochim. Biophys. Acta* 1015, 141–149.

Diner, B. A., & de Vitry, C. (1995) in *Advances in Photosynthesis Research*, Vol. 1 (Sybesma, C., Ed.) pp 407–411, Martinus Nijhoff/Dr. W. Junk, The Hague.

Diner, B. A., Petrouleas, V., & Wendolski, J. J. (1991) *Physiol. Plant* 81, 423–436.

Dismukes, G. C. (1986) *Photochem. Photobiol.* 43, 99–115.

Dismukes, G. C., & Siderer, Y. (1981) *Proc. Natl. Acad. Sci. U.S.A.* 78, 274–278.

Friso, G., Spetea, C., Giacometti, G. M., Vass, I., & Barbato, R. (1993) *Biochim. Biophys. Acta* 1184, 78–84.

Friso, G., Barbato, R., Giacometti, G. M., & Barber, J. (1994) *FEBS Lett.* 339, 217–221.

Gerken, S., Brettel, K., Schlodder, E., & Witt, H. T. (1988) *FEBS Lett.* 237, 69–75.

Gilchrist, M. L., Ball, J. A., Jr., Randall, D. W., & Britt, R. D. (1995) *Proc. Natl. Acad. Sci. U.S.A.* 86, 9545–9549.

Greenberg, B. M., Gaba, V., Canaani, O., Malkin, S., Mattoo, A. K., & Edelman, M. (1989a) *Proc. Natl. Acad. Sci. U.S.A.* 86, 6617–6620.

Greenberg, B. M., Gaba, V., Mattoo, A. K., & Edelman, M. (1989b) *Z. Naturforsch.* 44c, 450–452.

Harm, W. (1980) in *Biological Effects of Ultraviolet Radiation*, Cambridge University Press, London.

Hideg, É., & Vass, I. (1995) *Plant Sci.* 115, 251–260.

Hideg, É., Sass, L., Barbato, R., & Vass, I. (1993) *Photosynth. Res.* 38, 455–462.

Hoganson, C. W., & Babcock, G. T. (1988) *Biochemistry* 27, 5848–5855.

Irrgang, K. D., Geiken, B., Lange, B., & Renger, G. (1992) in *Research in Photosynthesis*, Vol. II (Murata, N., Ed.) pp 417–420, Kluwer, Dordrecht.

Jones, L. W., & Kok, B. (1966a) *Plant Physiol.* 41, 1037–1043.

Jones, L. W., & Kok, B. (1966b) *Plant Physiol.* 41, 1044–1049.

Kerr, J. B., & McElroy, C. T. (1993) *Science* 262, 1032–1034.

Melis, A., Nemson, J. A., & Harrison, M. A. (1992) *Biochim. Biophys. Acta* 1100, 312–320.

Michel, H., & Deisenhofer, J. (1986) in *Photosynthesis III: Photosynthetic Membranes and Light-Harvesting Systems. Encyclopedia of Plant Physiology. New Series Vol. 19* (Staehelin, L. A., & Arntzen, C. J., Eds.) pp 371–381, Springer, Berlin.

Miller, A.-F., & Brudvig, G. W. (1991) *Biochim. Biophys. Acta* 1056, 1–18.

Miyao, M., & Murata, N. (1984) *FEBS Lett.* 170, 350–354.

- Nanba, O., & Satoh, K. (1987) *Proc. Natl. Acad. Sci. U.S.A.* 84, 109–112.
- Nugent, J. H. A., Diner, B. A., & Evans, M. C. W. (1981) *FEBS Lett.* 124, 241–244.
- Ono, T. A., & Inoue, Y. (1984) *FEBS Lett.* 168, 281–286.
- Petrouleas, V., & Diner, B. A. (1986) *Biochim. Biophys. Acta* 849, 264–275.
- Renger, G. (1978) in *Photosynthetic Water Oxidation* (Metzner, H., Ed.) pp 229–248, Academic Press, London.
- Renger, G., Voss, M., Graber, P., & Schulze, A. (1986) in *Stratospheric Ozone Reduction, Solar Ultraviolet Radiation and Plant Life* (Worrest, C., & Caldwell, M. M., Eds.) pp 171–184, Springer, Berlin.
- Renger, G., Völker, M., Eckert, H. J., Fromme, R., Hohm-Veit, S., & Graber, P. (1989) *Photochem. Photobiol.* 49, 97–105.
- Rontó, Gy., Fekete, A., Gápar, S., & Módos, K. (1989) *J. Photochem. Photobiol. B3*, 497–507.
- Rutherford, A. W., & Zimmermann, J.-L. (1984) *Biochim. Biophys. Acta* 767, 168–175.
- Smith, R. C., Prézélin, B. B., Baker, K. S., Bidigare, R. R., Boucher, N. P., Coley, T., Karentz, D., MacIntyre, S., Matlick, H. A., Menzies, D., Ondrusek, M., Wan, Z., & Waters, K. J. (1995) *Science* 255, 952–959.
- Spetea, C., Hideg, É., & Vass, I. (1995) *Plant Sci.* 115, 207–215.
- Stolarski, R., Bojkov, R., Bishop, L., Zeferos, C., Staehelin, J., & Zawodny, J. (1992) *Science* 256, 342–349.
- Styring, S., Virgin, I., Ehrenberg, A., & Andersson, B. (1990) *Biochim. Biophys. Acta* 1015, 269–278.
- Tanada, S., & Wada, K. (1988) *Photosynth. Res.* 17, 255–266.
- Tevini, M. (1993) in *UV-B radiation and ozone depletion. Effects on Humans, Animals, Plants, Microorganisms, and Materials* (Tevini, M., Ed.) pp 1–15, Lewis Publishers, Boca Raton, Ann Arbor, London, Tokyo.
- Tevini, M., & Pfister, K. (1984) *Z. Naturforsch.* 40c, 129–133.
- Thompson, L. K., Miller, A.-F., Buser, C. A., De Paula, J. C., & Brudvig, G. W. (1989) *Biochemistry* 28, 8048–8056.
- Trebst, A. (1986) *Z. Naturforsch.* 41c, 240–244.
- Trebst, A., & Depka, B. (1990) *Z. Naturforsch.* 45c, 765–771.
- Vass, I., Cook, K. M., Deák, Zs., Mayes, S. R., & Barber, J. (1992) *Biochim. Biophys. Acta* 1102, 195–201.
- Vass, I., Sanakis, Y., Spetea, C., & Petrouleas, V. (1995) *Biochemistry* 34, 4434–4440.
- Vermaas, A. F. J., & Rutherford, A. W. (1984) *FEBS Lett.* 175, 243–248.
- Virgin, I., Styring, S., & Andersson, B. (1988) *FEBS Lett.* 233, 408–412.
- Vladimirov, Y. A., Roshchupkin, D. I., & Fesenko, E. E. (1970) *Photochem. Photobiol.* 11, 227–246.
- Wydrzynski, T., Angström, I., & Vanngard, T. (1989) *Biochim. Biophys. Acta* 973, 23–28.
- Yerkes, C. T., Kramer, D. M., Fenton, J. M., & Crofts, A. R. (1990) in *Current Research in Photosynthesis, Vol. II* (Baltcheffsky, M., Ed.) pp II.6.381–II.6.384, Kluwer Academic Publishers, Dordrecht, The Netherlands.
- Zimmermann, J. L., & Rutherford, A. W. (1984) *Biochim. Biophys. Acta* 767, 160–167.

BI9530595